

Experimental data on the reflection and transmission spectral response of photocathodes

R. J. Brooks, J. R. Howorth, K. McGarry and J. R. Powell

Photek Limited, 26 Castleham Road, St Leonards on Sea, East Sussex, TN38 9NS, United Kingdom

C.L. Joseph

Rutgers University, The State University of New Jersey, 136 Frelinghuysen Rd., Piscataway, NJ 08854, USA

ABSTRACT

The spectral transmission and electron emissivity responses, measured for a series of typical photocathodes, are presented and analysed. Specifically, samples of S1, S20, S25, Bialkali and two types of solar-blind telluride photocathodes were investigated in both transmission and reflection modes of operation. The transmission mode is more convenient for imaging, night vision and for scintillation counting applications such as CT scanners and is more commonly used than the reflection mode. However, more recent work has focussed on the reflection photocathode as a source of electrons with low energy spread used for electron guns for microscopy and lithographic free electron lasers [1]. Our analysis provides a determination of the reflectivity of the substrate/cathode and cathode/vacuum interface, enabling the refractive index to be deduced. The high apparent quantum efficiency (QE) of some conventional photocathodes is shown to be due to the conversion of each photon to two or more electrons.

KEYWORDS: Photocathode, solar-blind, S20, bialkali, S1,

1. INTRODUCTION

There are a number of papers that describe the photosensitivity of the various standard photocathodes in either: reflection mode (electrons emitted backwards from the illuminated photoemissive surface) or transmission mode (the illumination passes through a transparent window into a photoemissive layer and the electrons emitted from the opposite surface).

The photocathode could also be deposited on a reflective metal surface, enabling very high instantaneous pulse currents and light not absorbed on the first pass was reflected back from the reflecting substrate for a second pass effectively doubling the optical absorption and quantum efficiency [2].

Photek participated in a European project to improve photocathodes for medical diagnosis. During our studies it was useful to build experimental test cells so that both modes of operation could be compared. This new tool allows many more measurements compared to a conventional photo-tube and therefore enables further analysis of the photocathode characteristics. Further, we needed to produce sensitive reflecting UV photocathodes for an EBCCD development in collaboration with Rutgers University. That project, funded through NASA, aimed to provide solar-blind high-QE UV detectors for space science missions.

2. EXPERIMENTAL MEASUREMENTS

The general design of an experimental test cell is shown in Figure 1A.

The biplanar diode has a window at each end. A photocathode is deposited on the inside of one window and an ITO coating on the other to collect and provide a conductive path for photoelectrons. The spectral response can be measured with the light input in either transmission mode (through the photocathode window) – or reflection mode (through the ITO window), with light incident on the vacuum side.

External mirrors can be placed near the windows to reflect light back through the device for a second pass. The optical transmission can also be measured directly.

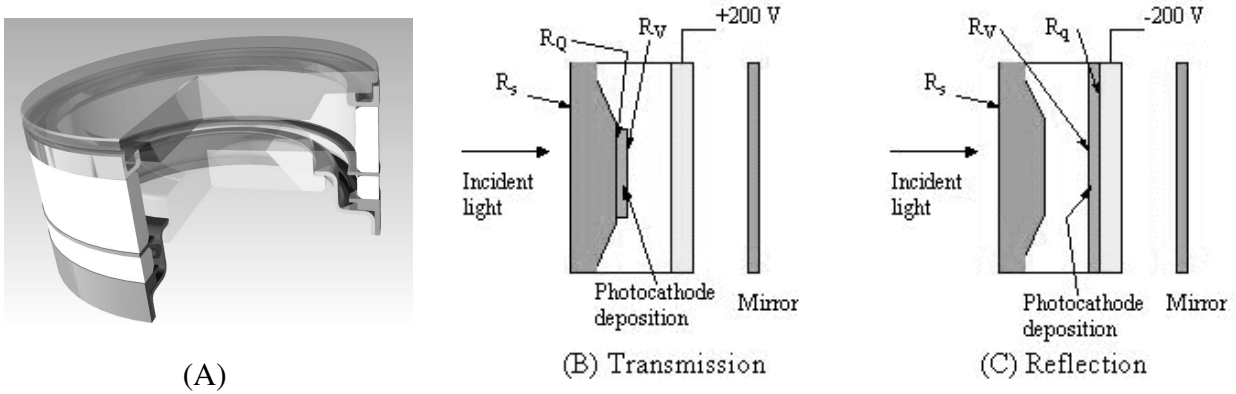


Figure 1: (A) Experimental test cell with photocathode window and rear window with ITO coating (or nickel mesh for UV cathodes) on inside surface for photo-electron collection. (B) Schematic test set up for transmission-mode testing showing the reflection interfaces, R_s , R_Q , and R_V . (C) Same as B, but for reflection measurements. The 200 V bias to ground is used to measure the photocurrent signals, S .

The cathodes are made in a remote process vacuum transfer system – two or more photocathodes fabricated in the same process have almost identical photo response, which allows useful studies of different substrate materials. Glass is used for visible response cathodes and fused silica or sapphire for UV cathodes: with a short wavelength cut-offs of 170 nm and 150 nm respectively. Magnesium fluoride (MgF_2) windows allow measurement down to 110nm for the Rutgers EBCCD project.

Concurrently with these projects, we were also making measurements to study the spatial resolution of proximity focus tubes with different photocathodes as a function of wavelength as part of the UVIT project for the Indian Space Research Organisation’s ASTROSAT mission. We reported on this in [3].

3. ANALYSIS

3.1 Transmission mode

A schematic diagram of a transmission mode photocathode is shown in fig 1B. The optical reflection (R_s) at the air / fused silica interface is about 4% from the refractive index of 1.5.

The widely used S-20 photocathode is known to have a refractive index in the range to 2.5 to 4.5 [4, 5, 6], with stronger reflectivity at the fused silica to photocathode interface (R_Q) and an even stronger reflection at the photocathode to vacuum interface (R_V). Consequently, the well-known interference colours can be seen on S-20 photocathodes of different thicknesses during S-20 photocathode fabrication.

The measured sensitivity (QE) of a transmission photocathode is, therefore, reduced by the initial reflection losses at the air-window interface, and at the window / cathode interface (R_s and R_Q). If the proportion of incident light absorbed in the photocathode is small, then the reflected light from the vacuum interface (R_V) can boost the measured sensitivity. If the fraction of light not absorbed in the first pass through the cathode is “ f ” we have:

$$S_{T\text{ meas}} = S(1 - R_s - R_Q) + fS R_V$$

If an external mirror is used to get 100% of the remaining photons for a second pass, we have:

$$S_{T\text{ mirror}} = S_{T\text{ meas}} + fS(1 - 4R_s - 2R_V)$$

The difference between these two measurements enables R_v to be deduced unambiguously at longer wavelengths (where absorption is poor), such that we can assume that $fS \approx S_{meas}$, for example:

$$S_T \text{ mirror} - S_T \text{ meas} = fS (1 - 4R_s - R_v)$$

$$\frac{S_T \text{ mirror} - S_T \text{ meas}}{fS} = 1 - 4R_s - R_v$$

$$R_v = 4R_s - \left(\frac{S_T \text{ mirror} - S_T \text{ meas}}{fS} \right) - 1$$

Knowledge of R_v allows the refractive index to be determined. The refractive index of air/vacuum = 1 therefore :

$$n = \left(\frac{1 + \sqrt{R_v}}{1 - \sqrt{R_v}} \right)$$

3.2 Reflection Mode

A schematic diagram of the photocathode operating in reflection mode is shown in figure 1C. In this case, the initial reflectivity R_v at the photocathode/vacuum interface can be rather high e.g., 25% if the refractive index of the cathode is 3. Light not absorbed by the photocathode is less likely to be returned for a second pass, as the reflectivity at the cathode/fused silica interface (R_q) is not large.

The corresponding formulae for S_R meas are:

$$S_R \text{ meas} = S (1 - 2R_s - R_v) + fS R_q$$

And with an external mirror:

$$S_R \text{ mirror} = S_R \text{ meas} + fS (1 - 4R_s - 2R_v)$$

A similar analysis to the transmission mode enables R_q to be determined and of course a second determination of the photocathode refractive index to be made.

$$S_R \text{ mirror} - S_R \text{ meas} = fS (1 - 4R_s - 2R_v)$$

$$\frac{S_R \text{ mirror} - S_R \text{ meas}}{S_R \text{ meas}} = 1 - R_q$$

$$R_q = - \left(\frac{S_R \text{ mirror} - S_R \text{ meas}}{S_R \text{ meas}} \right) - 1$$

4. EXPERIMENTAL RESULTS

The spectral response for each different photocathode was obtained; figure (2) shows the S20 response as an example. The key data are tabulated in (Table1) and are consistent with the high photocathode refractive index. In general, the reflection sensitivity is much lower than the transmission sensitivity due to the high optical reflectivity of the

vacuum/photocathode interface. Our results stand in stark contrast with those for short-wavelength UV photocathodes such as CsI or KBr, where the strong absorption coefficients favour opaque, reflective cathodes over semitransparent ones. In addition, the QE of CsTe at 11 eV (~150 nm) can be above 60% [7] and even higher shortward.

In the present study an external mirror was always used to return light to the photocathode for a second pass and had a relatively large impact on QE. Image intensifiers built with proximity focus to a microchannel plate (MCP) automatically benefit from this effect with the MCP reflecting about 40% of the light transmitted by the cathode for a second pass. While enhancing the photo-response this light is not optimally focussed, degrading somewhat the MTF of the image intensifier.

It is also interesting to note that the use of a mirror gives a greater enhancement in the reflective mode. In the present studies, the reflectivity, R_v , of the cathode/vacuum interface is relatively high, whereas R_Q , the reflectivity of the cathode to fused silica interface is relatively small.

Obviously, there can be more than one reflection back through the optical system when using a mirror. These reflections will become smaller in magnitude as the light is transmitted out of and absorbed by the system so as to eventually become negligible. This will happen rapidly in transmission mode as significant light is lost at the vacuum to photocathode interface. In the reflection mode however, this same interface works to reflect the light back through the photocathode towards the mirror. There are differences in the refractive index measured in transmission and reflection mode. We attribute this partly to the above effect, partly to the non-zero absorption of the photocathode itself and also due to experimental error in each of the spectral measurements. This could be 5% on each of the four measurements made at each wavelength.

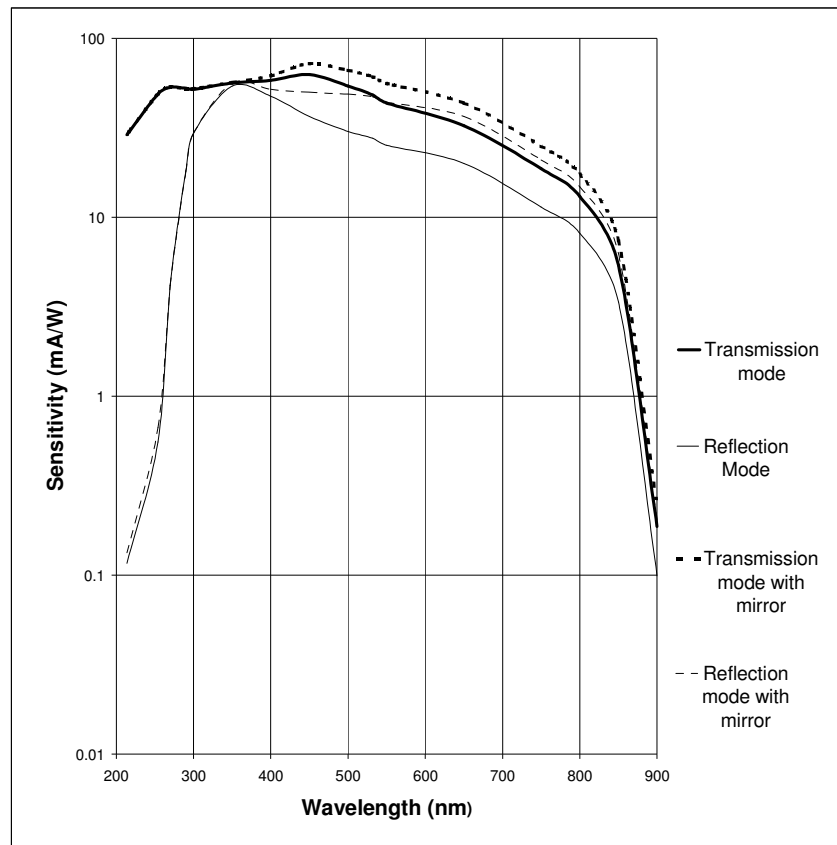


Figure 2: Spectral response of S20 photocathode (serial: TC81030225) in transmission and reflection mode. The poor response of the reflection mode in the UV is due to transmission losses in the rear window. The calculations for refractive index are based on long wavelengths where the transmission losses and cathode absorption are low.

Photocathode	S20	S25	KCsSb	KcsTe	RbCsTe	S1
Serial Number	8103 0225	8203 0926	8103 0411	1305 0512	1305 0823	7104 0116
$(S_T \text{ Mirror} - S_T \text{ Meas}) / S_T \text{ Meas}$	0.33	0.11	0.5	0.27	0.6	0.125
Rv	0.26	0.37	0.17	0.29	0.24	0.36
n	3.1	4.1	2.4	3.3	2.92	4.0
$(S_R \text{ Mirror} - S_R \text{ Meas}) / S_R \text{ Meas}$	0.75	0.64	0.17	0.29	0.62	0.75
Rq	0.13	0.18	0.42	0.36	0.19	0.4
n	2.1	2.5	4.7	4	2.5	4.4

Table 1: Reflection and refractive index measurements from a variety of different types of photocathode in transmission and reflection mode

5. SPECIFIC RESULTS OF THE VARIOUS PHOTOCATHODES

5.1 The S20/S25 Photocathodes

The S20 photocathode is one of the newest, accidentally discovered by Sommer in 1956 [8]. Thicker layers of the same materials have higher IR response, lower blue response and are designated S25. The S25 photocathode has been made in huge quantities – probably some millions of individual tubes for military night vision applications.

As the Sodium – Potassium – Antimony layers are thickened – up during deposition, the colour of the cathode changes like any other interference filter from nothing, to blue, to green etc. This is illustrated in our Figure 82030926/S20 and 81030225/S20 as rather thicker versions of S20, but not yet with S25 characteristics. Both cathodes have clear peaks in transmission mode at 450 nm and 260 nm. It can be seen that for wavelengths beyond 400 nm, the response can be increased by a factor of 1.25 to 1.5 by placing a mirror behind the cathode to return light for a second pass through the cathode. It is clear, that these cathode samples were efficient absorbers at wavelengths below 400 nm.

In reflection mode, the sensitivity is typically half of that in transmission mode, due to the high optical reflectivity at the vacuum/photocathode interface. The transmission-mode photocathode gains an almost equal amount as the reflection cathode loses, as the light not absorbed during the first pass is partially reflected at the cathode/vacuum interface. An external mirror increases the reflection sensitivity to close to the transmission mode case in the 400-900 nm region.

In the UV, the sensitivity of the reflection mode photocathode peaks at over 30% at 270 nm. Taking account of the photon losses at the vacuum/cathode interface, the S20 cathode converts 45-60% of photons into photo-electrons.

Our reflectivity measurements show the refractive index of our S20 photocathodes averaged about 4.1. This can be compared with previously published values of 2.9 [4] and 3.7 [5]. At wavelengths below 400 nm, the S20 cathode is very absorptive, as shown in our experiments with mirrors, but the QE falls to a valley, before rising to a secondary peak in the UV at circa 250 nm. Below 400 nm, there is an increasing probability that a photon can generate two electrons. At 400 nm (3 eV) these electron pairs could average 1.5 eV, only slightly above the threshold/work function. Such electrons have low escape probability, explaining the QE valley at about 350 nm. At 250 nm, the photon energy approaches 5 eV, producing pairs of electrons, each with high excess energy compared to the work function of c.1.4 eV. This explains the

high QE in the UV as well as the minimum around 300 nm (two low-energy electrons). This hypothesis is not new; our work reinforces earlier work published by [7,9]

The radial electron energy distribution as determined by spatial resolution/point spread function corroborates this evidence. This should be simply a function of photo energy less work function and one would expect the spatial resolution to degrade continuously with increasing photon energy. In fact, spatial resolution improves in the region between 300nm and 250 nm, before it starts to degrade again as photon energy approaches 6 eV. This work is described in [3].

5.2 Bialkali Photocathodes

The term – “bialkali photocathode” is rather imprecise and is commonly used to describe Sodium – Potassium – Antimony – closely related to the S20 described in 5.1, Rubidium – Caesium – Antimony [10] and Potassium – Caesium – Antimony [11]. Our test cell indicates that the sample was rather thin, with incomplete optical absorption at wavelength longer than 350 nm and a high refractive index. There is also some indication of two electrons generated per photon at wavelengths below 250 nm as reported by Sobieski [12].

5.3 Solar Blind (Telluride) Photocathodes

The earliest reference to Telluride photocathodes is E A Taft & L Apker [13]. Tellurium is closely related to Antimony in the Periodic Table, so the mono-alkalis, Cs, Rb & K Te are all viable. Sodium could be another alternative.

We have investigated the bialkali compounds – CsRbTe, and KCsTe. The latter is frequently discussed in the literature [14] for applications as an electron source for electronography etc. Bialkali types have better QE than the mono-alkali telluride photocathodes.

Photo tubes remain important at short wavelengths of the UV spectrum, because they have higher sensitivity than semiconductor devices and behave as efficient optical filters, rejecting longer wavelength photons making them “solar-blind”.

There is a strong incentive to improve the UV photocathode. Fig (3) shows the spectral response of the MAMA tube on STIS, and the spectral curve of an experimental tube with reflective photocathode, made for Rutgers University.

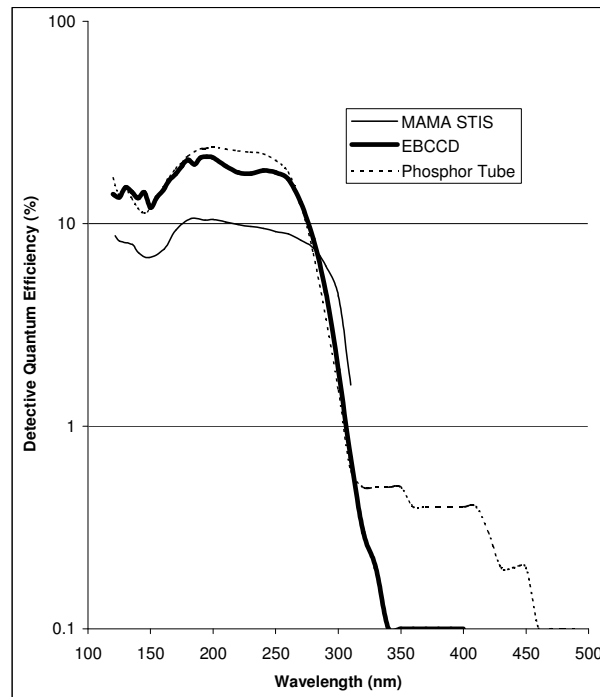


Figure (3) Comparison of detective quantum efficiency of the Photek EBCCD tube built for Rutgers University with the STIS MAMA detector. A variant of the Photek tube using a phosphor screen instead of an EBCCD is also shown.

Transmission curves shown here in Figure (4) are not compensated for the transmission loss of the (MgF_2) input window, indicating the internal QE of the photocathode is 20-30% at 120 nm. Initially, we had anticipated that the solar blind cathode would be very transparent down to wavelengths as short as 300 or 350 nm. Our data, however, shows that in fact, the absorption starts to rise at wavelengths shorter than 450 nm and tends to peak around 280 nm figure (4), which is where the sensitivity also peaks.

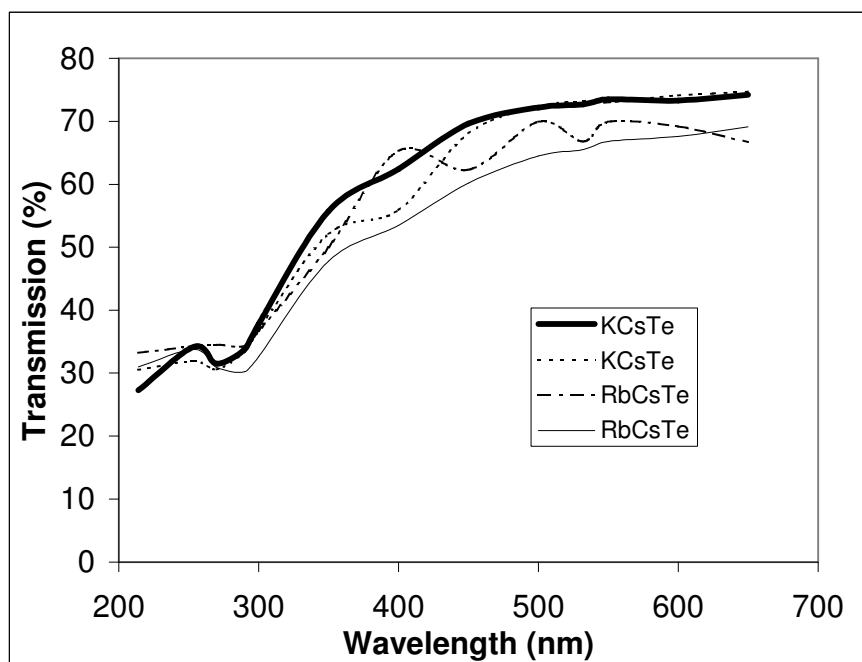


Figure (4) Transmission results as a function of wavelength for telluride photocathodes on a test cell with a sapphire rear window. The entrance window was MgF_2 . Tubes 13050823 and 13060223 were RbCsTe, the other two were KCsTe.

This may well be followed by a second rise in absorption at shorter wavelengths, but strong absorption in the window materials makes this speculative. The sharp cut-off in the spectral response curves at wavelengths above 300 nm therefore is not purely driven by optical absorption.

The bandgap appears to be in the range 2.7 – 2.9 eV and these photoelectrons have a poor chance of escaping over a higher work function barrier. It seems that at wavelengths below 200 nm, the photons have sufficient energy to generate two electrons, both of which have a low probability of escaping over the 3.5 eV barrier. The QE consequently drops to a minimum at about 160 nm (7.6 eV). At shorter wavelength than this, both photoelectrons have sufficient energy to escape easily, and the QE starts to rise. The MgF_2 window short wavelength cut-off masks its extent and magnitude. Powell [7] reports that the QE of CsTe can be above 60% @11eV. They also deduce a bandgap of 3eV, close to our figure for the RbCsTe bialkali.

Our optical data shows that the refractive index of KC_3Te is between 4 and 4.5, very similar to KC_3Sb , while RbC_3Te has a lower refractive index of approximately 2.5. Consequently, the QE of this type of cathode is better enhanced than alternatives by the mirror to providing a second absorption pass. The optical absorption is quite weak. The absence of any colour or visible interference colour supports the view that both optical absorption and reflectivity at the cathode/vacuum interface are low.

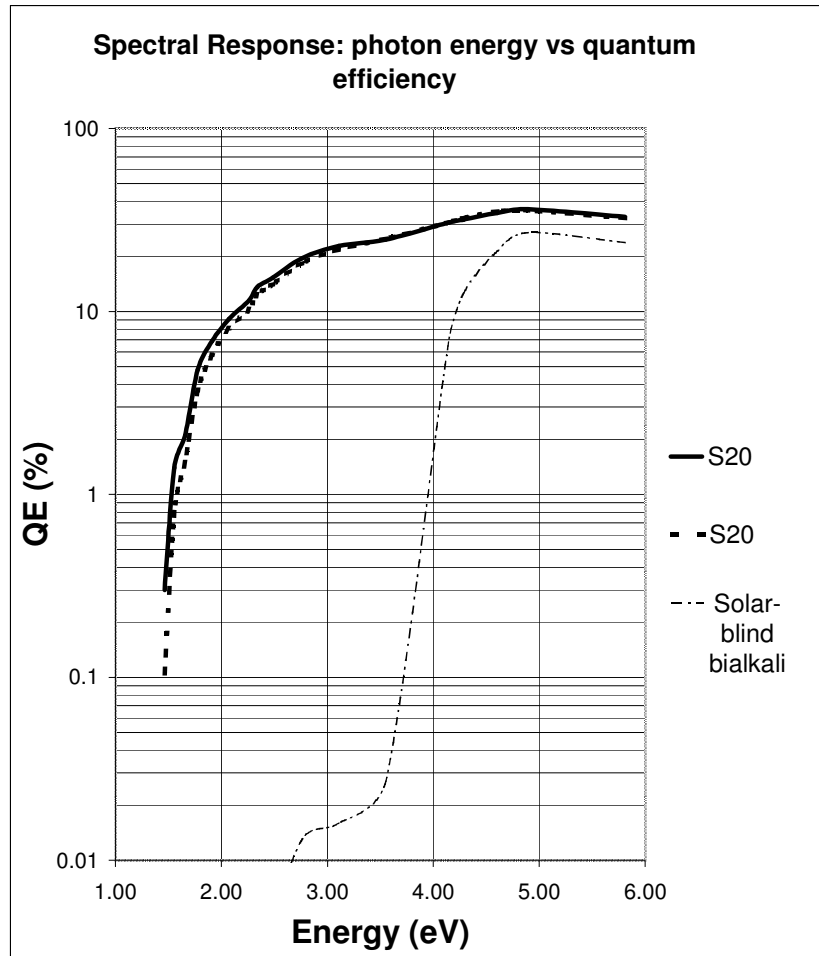


Figure (5) shows the spectral response of two S20 tubes and a solar blind tube plotted as quantum efficiency as a function of photon energy. The responses tend to peak at around 4.8eV.

5.4 The S1 Photocathode

The S1 photocathode was developed in 1929. There is a mass of literature about it, but data on its reflectivity and refractive index is difficult to find. Our data (Table 1) shows that it is highly reflective, with a refractive index of between 4 and 4.4. It could be argued that there was a significant proportion of metallic silver in the photocathodes. The optical transmission of the cathode was also measured, figure (5). This is quite remarkable and we are unable to suggest a model for its behaviour.

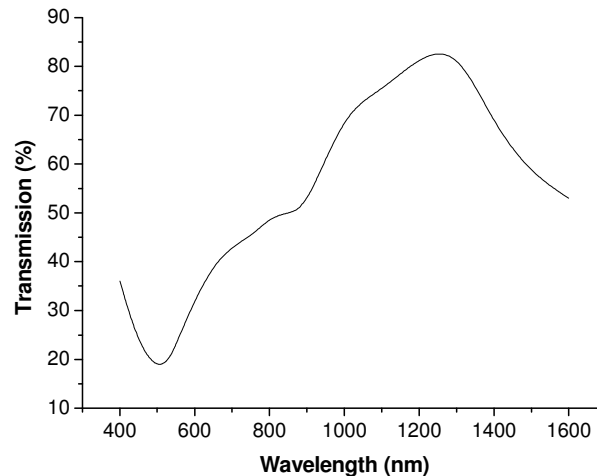


Figure (6) Transmission of S-1 photocathode as a function of wavelength

6. SUMMARY

The present study permits a separation of key parameters associated with the fabrication of important photocathodes, especially those used for wavelengths longward of 160 nm. Our results enable better optimisation of quantum efficiencies in these photoemissive systems.

7. REFERENCES

- 1) "Photocathodes for Free Electron Lasers", SH Kong, J Kimross-Wright, DC Nguyen and RL Sheffield, *Nuc Inst. & Methods A*, 258, 272-275 (1995)
- 2) Novice M. A. and Vine J. "Optical Means for Enhancing the Sensitivity of a Tri-Alkali Photocathode", *Appl. Opt.* 6, 7, 1171-1175 (1967)
- 3) "Wavelength-Dependent Resolution and Electron Energy Distribution Measurements of Image Intensifiers" R Brooks, M Ingle, J Milnes, J Howorth, J Hutchings: *Proc. SPIE Vol. 6294, 62940W* (Sep. 7, 2006)
- 4) "Optical Means For Enhancing The Sensitivity of a Tri Alkali Photocathode" MA Novice and J Vine *Appl. Opt.* 6, 1171-1178 (1967)
- 5) "Contribution a L'Optimisation des Photocathodes Trialcalines Semi-Transparentes", G Eschard and P Dolizy, *J. de Physique*, 34, C6-61, 1973
- 6) "Enhanced Sensitivity and Speed in Photomultiplier Tubes", S Hallensleben, D.Phil Thesis, University of Sussex, UK (2000)
- 7) "Photoemission Studies of Cesium Telluride", RA Powell, WE Spicer, GB Fisher and P Gregory, *Phys. Rev. B*, 8, 3987-3995
- 8) AH Sommer, *IRE Trans Nucl Sci* 3 8 1956
- 9) "Some Ultraviolet Spectral Sensitivity Characteristics of Broadband Multi-Alkali Photocathodes" CB Johnson, Bonney & RF Floryan, *SPIE* 932, 285-290 (1988)
- 10) "Technique For Producing High-Sensitivity Rubidium-Cesium-Antimony Photocathodes" C Morrison, *J. Appl. Phys.* 37, 713-715 (1966)
- 11) "Band-Bending Effects in Na₂K₂Sb and K₂CsSb" DG Fisher, AF McDonie and AH Sommer, *J. Appl Phys.* 45, 487-488 (1974)
- 12) "Ultraviolet Response of Semi-Transparent Multi-Alkali Photocathodes" S Sobieski, *Appl. Opt.* 15, 2298-99 (1976)
- 13) Taft & Apker *JOSA* 43 81-1953.
- 14) "Technological Challenges for High Brightness Photo-Injectors", G Subberluq, CERN, Geneva, CARE Conference -04-029, PHIN